Journal of Histochemistry & Cytochemistry 2014, Vol. 62(5) 369–388

DOI: 10.1369/0022155414528514
jhc.sagepub.com
SAGE

Brain Barriers and a Subpopulation of Astroglial Progenitors of Developing Human Forebrain Are Immunostained for the Glycoprotein YKL-40

Camilla Bjørnbak,[1] Christian B. Brøchner,[1] Lars A. Larsen, Julia S. Johansen, and Kjeld Møllgård

Department of Cellular and Molecular Medicine (CB,CBB,LAL,KM); Department of Clinical Medicine (JSJ), Faculty of Health and Medical Sciences, University of Copenhagen, Blegdamsvej 3, DK-2200 Copenhagen, Denmark; Departments of Medicine and Oncology (JSJ), Herlev Hospital, Copenhagen University Hospital, Copenhagen, Denmark (JSJ)

Summary

YKL-40, a glycoprotein involved in cell differentiation, has been associated with neurodevelopmental disorders, angiogenesis, neuroinflammation and glioblastomas. We evaluated YKL-40 protein distribution in the early human forebrain using double-labeling immunofluorescence and immunohistochemistry. Immunoreactivity was detected in neuroepithelial cells, radial glial end feet, leptomeningeal cells and choroid plexus epithelial cells. The subpial marginal zone was YKL-40-positive, particularly in the hippocampus, from an early beginning stage in its development. Blood vessels in the intermediate and subventricular zones showed specific YKL-40 reactivity confined to pericytes. Furthermore, a population of YKL-40-positive, small, rounded cells was identified in the ventricular and subventricular zones. Real-time quantitative RT-PCR analysis showed strong YKL-40 mRNA expression in the leptomeninges and the choroid plexuses, and weaker expression in the telencephalic wall. Immunohistochemistry revealed a differential distribution of YKL-40 across the zones of the developing telencephalic wall. We show that YKL-40 is associated with sites of the brain barrier systems and propose that it is involved in controlling local angiogenesis and access of peripheral cells to the forebrain via secretion from leptomeningeal cells, choroid plexus epithelium and pericytes. Furthermore, we suggest that the small, rounded, YKL-40-positive cells represent a subpopulation of astroglial progenitors, and that YKL-40 could be involved in the differentiation of a particular astrocytic lineage. (J Histochem Cytochem 62:369–388, 2014)

Keywords

astrocytes, brain barriers, cerebral cortex, development, neural stem cells

Introduction

YKL-40, also named chitinase 3-like 1 (CHI3L1), a member of mammalian chitinase-like proteins, is a heparin-, chitin- and collagen-binding glycoprotein without chitinase activity (Hakala et al. 1993; Bigg et al. 2006). The interleukin receptor, IL-13Rα2, was recently identified as a receptor for YKL-40, but other receptors may also exist (He et al. 2013). YKL-40 is a highly conserved glycoprotein mainly produced by fetal and embryonic stem cells, neutrophils, macrophages, reactive astrocytes and cancer cells (Rehli et al. 1997; Volck et al. 1998; Junker et al. 2005; Johansen et al. 2009; Horbinski et al. 2010; Brøchner et al. 2012). YKL-40 stimulates the production of vascular endothelial growth factor (VEGF), and plays a role in angiogenesis (Faibish

Received for publication December 16, 2013; accepted February 24, 2014.

[1]These authors contributed equally to this work.

Corresponding Author:
Kjeld Møllgård, Professor, MD, PhD, Department of Cellular and Molecular Medicine, The Panum Institute, Blegdamsvej 3, DK-2200 Copenhagen.
E-mail: kjm@sund.ku.dk

et al. 2011; Francescone et al. 2011; Shao 2013), inflammation (Recklies et al. 2005; Lee et al. 2011) and cellular proliferation and differentiation (Johansen et al. 2007; Brøchner et al. 2012).

YKL-40, Neuroinflammation and the Brain Barrier System

Plasma YKL-40 is emerging as a new biomarker for disease severity and poor prognosis in patients with cancer and diseases characterized by inflammation and tissue remodeling (Johansen et al. 2009; Johansen et al. 2010; Kjaergaard et al. 2010). YKL-40 is increased in the cerebrospinal fluid of patients with multiple sclerosis (MS) (Bonneh-Barkay et al. 2010) and purulent meningitis (Østergaard et al. 2002). In vivo, YKL-40 transcription in the brain is associated with astrocytes in MS and simian immunodeficiency virus encephalitis (SIVE; pigtailed macaque) and possibly also with Alzheimer's disease, amytrophic lateral sclerosis, autism, Pick's disease and schizophrenia (Chung et al. 2003; Colton et al. 2006; Garbett et al. 2008; Bonneh-Barkay et al. 2010). Bonneh-Barkay et al. also propose that YKL-40 is correlated with reactive gliosis, particularly in response to neuroinflammation Bonneh-Barkay et al. 2010). Accumulated work in the field suggests that neuroinflammation is of great importance in almost all neurological disorders, and that interactions between the brain barriers and the immune system contribute to this process (Stolp et al. 2013).

In a study of YKL-40 expression in developing human embryonic and fetal tissues, YKL-40 was found to be associated with tissues undergoing morphogenetic changes (Johansen et al. 2007). We showed unique mRNA expression of *YKL-40* in the human fetal choroid plexus (Johansen et al. 2007), a prominent part of the brain barrier system involved in the process of neuroinflammation (Stolp et al. 2013). The distribution of YKL-40 in the developing human forebrain and its possible role in brain barrier sites is unknown.

YKL-40, Glioblastomas and Neural Stem Cells

YKL-40 plasma levels are elevated in 55–75% of patients with glioblastoma as compared with healthy subjects (Hormigo et al. 2006; Iwamoto et al. 2011; Bernadi et al. 2012). Following surgery for glioblastoma and anaplastic glioma, plasma levels of YKL-40 are lower in patients with no radiographic evidence of disease as compared with patients with radiographic evidence, and results suggest that increases in YKL-40 plasma concentrations during the follow-up are associated with shorter survival times (Iwamoto et al. 2011). Microarray gene analyses have shown that *YKL-40* is overexpressed in glioblastoma multiforme, as compared with normal tissue (Lal et al. 1999; Markert et al. 2001; Tanwar et al. 2002; Shostak et al. 2003; Nigro et al. 2005; Ku et al. 2011). Tumor stem cells may be involved in the initiation of gliomas and bear a resemblance to neural stem cells (Schiffer et al. 2010), which are present during the early development of the brain. In an earlier study, we have found a differential expression of YKL-40 in human embryonic stem cells and in cell progeny of the three germ layers, including the neuroectoderm (Brøchner et al. 2012). Given the association between YKL-40 and glioblastoma, YKL-40 is an intriguing possible marker of human neural stem cells or their progenitors.

YKL-40 in the Early Developing Human Forebrain

Studying the complex development of the human fetal cerebral cortex is impeded by obvious difficulties—for example, applying cell fate mapping—and therefore lags behind studies of nonhuman mammals (Bystron et al. 2008; Howard et al. 2008). Extrapolating directly from rodents to humans is not without risk, as human neocortical complexity far exceeds that of rodents. Hence, findings based on human samples are very important in order to understand normal brain development and disorders of the central nervous system.

So far, YKL-40 has been described particularly in diverse pathological conditions and promoted as a factor with profound implications for both diagnostic and therapeutic applications (Prakash et al. 2013), whereas the general role of YKL-40 in developmental biology has been largely ignored, with a few exceptions (Johansen et al. 2007; Brøchner et al. 2012). In order to elucidate its possible functions during brain development, we have focused on YKL-40 protein and its mRNA expression in human embryonic and fetal forebrain. Using immunohistochemical, double-labeling immunofluorescence and mRNA analysis, we describe the spatiotemporal appearance and distribution of YKL-40 in human forebrain from the 6th to the 21st week post-conception (wpc).

Materials & Methods

Tissue Samples

Nine human embryos (6th week, n=2; 7th, n=2; 8th, n=5) and 35 fetuses (9th week, n=3; 10th, n=2; 11th, n=3; 12th, n=3; 13th n=2; 14th, n=6; 15th, n=4; 16th, n=4; 17th, n=2; 18th, n=2; 19th, n=1; 20th, n=1; 21st, n=2) were examined immunohistochemically. Two human embryos (7th week, n=1; 8th, n=1) and three human fetuses (9th week, n=2; 10th, n=1) were used for real-time quantitative RT-PCR analysis. The embryos and fetuses ranged from 7 to 200 mm in crown-rump length (CRL), corresponding to 6th–21st wpc. The samples were obtained either from the archives of the human embryonic/fetal biobank, Department of Cellular and Molecular Medicine at the University of Copenhagen

or from legal abortions. According to the Helsinki declaration II, oral and written information was given and informed consent was obtained from all contributing women, according to and approved by the Research Ethics Committee of the Capital Region (KF–V.100.1735/90).

Immediately following surgery, the samples were either dissected into blocks and fixed for 12–24 hr at 4C in either 10% neutral-buffered formalin, 4% Formol-Calcium, Lillie's or Bouin's fixatives or, alternatively, carefully isolated and stored in RNAlater for subsequent PCR analysis. The specimens intended for immunohistochemistry were dehydrated with graded alcohols, cleared in xylene, and embedded in paraffin. Serial sections, 3–10-µm thick, were cut in transverse, sagittal or horizontal planes and placed on silanized glass slides.

Immunohistochemistry

Sections were deparaffinized and rehydrated in xylene followed by a series of graded alcohols, treated with a 0.5% solution of hydrogen peroxide in methanol for 15 min to quench endogenous peroxidase, and then rinsed in Tris-buffered saline (TBS, 5 mM Tris-HCl, 146 mM NaCl, pH 7.6). Non-specific binding was inhibited by incubation for 30 min with blocking buffer (ChemMate antibody diluent S2022; DakoCytomation, Glostrup, Denmark) at room temperature. The sections were incubated overnight at 4C with a mouse monoclonal antibody against human YKL-40 (201.F9, IgG2bκ, epitope GAWRGTTGHHS corresponding to amino acids 210–220 at a 1:50–1:100 dilution of the 1.9 mg/ml stock concentration in blocking buffer (ChemMate antibody diluent S2022)). The sections were washed with TBS and incubated for 30 min with a peroxidase-labeled polymer conjugated to goat anti-mouse immunoglobulins (DAKO EnVision™+ System/HRP K4007, DakoCytomation). The sections were washed with TBS and incubated for 10 min with 3,3'-diamino-benzidine chromogen solution. Positive staining was recognized as brown staining. The sections were counterstained with Mayer's hematoxylin and dehydrated in graded alcohols followed by xylene and coverslipped with DPX mounting media. Staining specificity was tested by preincubating the 201.F9 monoclonal antibody with purified human YKL-40 for 2 hr at room temperature or overnight at 4C to block YKL-40 binding sites and reveal possible nonspecific staining to the sections. The preabsorbed sections showed a lack of or a diminished reactivity (Fig. 1), which is in accordance with previously described results (see Figure 1 in Johansen et al. 2007). Positive controls included staining of tissue known to be immunoreactive for YKL-40 (Johansen et al. 2007). Non-immune mouse IgG1 (X0931, IgG1 concentration 7.5 µg/ml, DakoCytomation) was used as a negative control.

Double immunolabeling was performed with antibodies against YKL-40 and von Willebrand Factor (vWF) or YKL-40 and glial fibrillary acidic protein (GFAP). Prior to staining, nonspecific binding was inhibited by incubation for 30 min with 0.2% casein (C-7078; Sigma-Aldrich, St. Louis, MO) at room temperature. The sections were absorbed in human serum (known donor) and then incubated at 4C overnight with a mixture of antibodies against YKL-40 (201.F9, IgG2bκ, mouse, 1:100 dilution of the 1.9 mg/ml stock concentration) and vWF (A0082, rabbit, 1:1200; DakoCytomation) diluted in 0.2% casein. Following this, endogenous peroxidase was quenched using 0.3% hydrogen peroxide for 15 min. Sections were incubated for 30 min at room temperature with Labelled Polymer –HRP anti-mouse (DakoCytomation, EnVision™+ System/HRP K4007) followed by Tyramid Signal Amplification with Alexa Fluor 488 Tyramide (T20912; Invitrogen, Molecular Probes, Carlsbad, CA) for 7 min at room temperature. Subsequently, the sections were incubated for 30 min at room temperature with biotin-SP-conjugated $F(ab')_2$ fragment donkey anti-rabbit antibodies (711-066-152, 1:200; Jackson ImmunoResearch Laboratories, West Grove, PA) followed by streptavidin-conjugated DyLight 594 (SA5594, 1:200; Vector Laboratories, Burlingame, CA). Finally, a nuclear counterstain with DAPI (D1306, 1:1000; Invitrogen) was added for 3 min, and the sections coverslipped. For double staining with antibodies against YKL-40 and GFAP, the sections were prepared as described above, and then incubated with antibodies against YKL-40 (1:50 dilution of the 1.9 mg/ml stock concentration) overnight at 4C. After staining for YKL-40, sections were incubated with an antibody against GFAP (Z0334, rabbit, 1:700; DakoCytomation) overnight, with secondary antibody and nuclear counterstaining performed as described above.

Fluorescent imaging was performed using a Zeiss Axioplan 2 microscope, and laser scanning confocal microscopy performed using a Carl Zeiss LSM 780 with a Plan-Apochromat 63/1.40 Oil DIC M27 objective and the following lasers and emission filters: for excitation of Alexa Fluor 488, a 488 nm argon laser with an emission filter of 493-590 (green fluorescence); for excitation of DyLight 594, an In *Tune* laser with an emission filter of 596-692 (red fluorescence). During image acquisition, a sequential scanning procedure through the z-axis of the double-labeled sections was applied covering a total depth of 9 µm. Confocal images were taken and analyzed throughout the z-axis of the section, and individual optical sections were stored as TIFF files using Zeiss ZEN Vision v10. Representative images for figure editing were chosen from the analyzed samples.

Real-time Quantitative RT-PCR Analysis

Tissue samples for mRNA analysis were placed in RNAlater (Ambion, Austin, TX) immediately after dissection and stored according to the manufacturers' instructions. Total

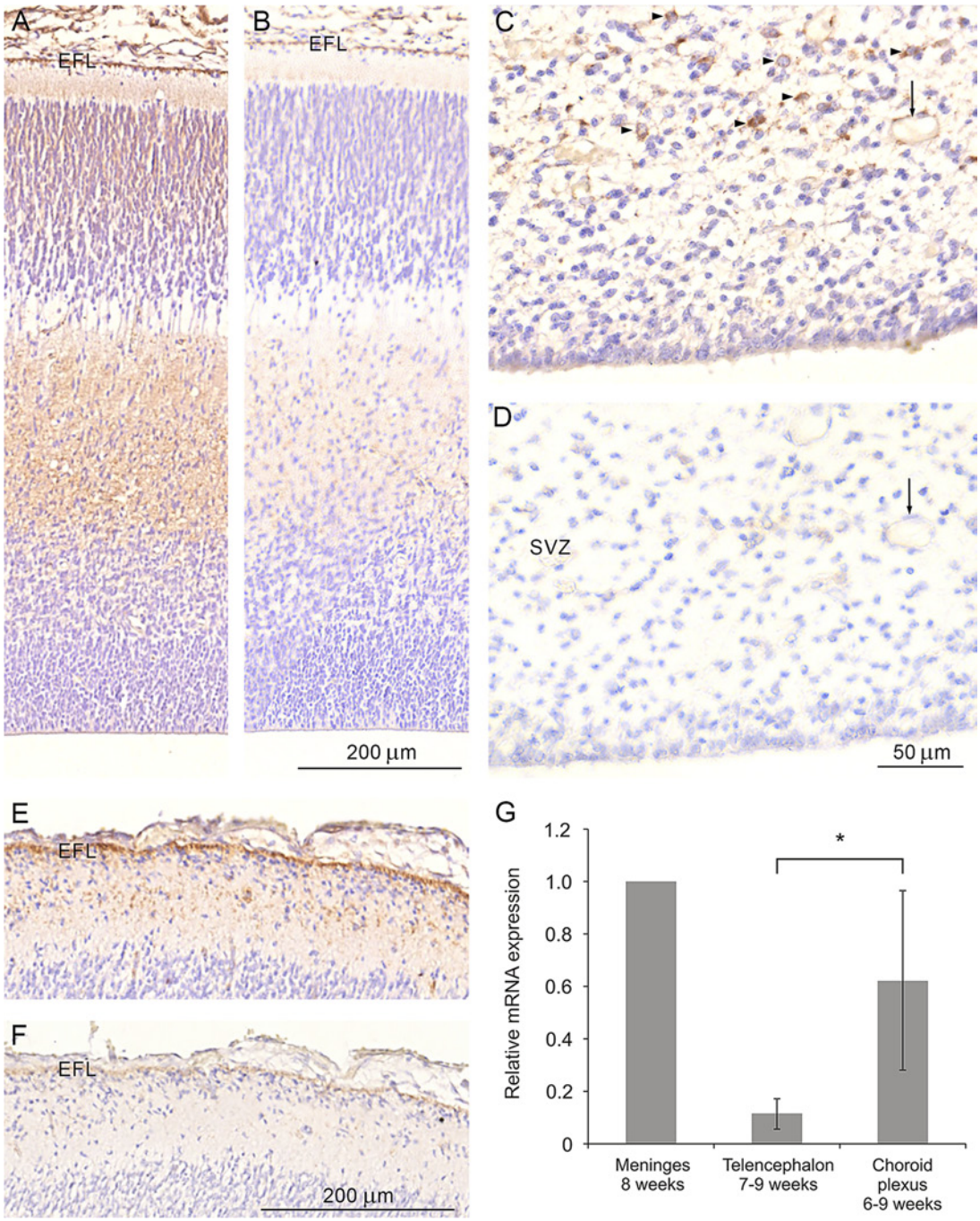

Figure 1. YKL-40 protein distribution in the neocortex of a human fetus at the 12th week post-conception (wpc) (CRL: 75 mm) (A-B**)**, and in the occipital cortex of a 21st wpc fetus (CRL: 200 mm) (C-F). Sections shown in (A), (C) and (E) were stained with the monoclonal antibody (MAb) 201.F9 whereas those in (B), (D) and (F) were stained using the MAb 201.F9 preabsorbed with purified human YKL-40 protein. Note the lack of or a markedly diminished reactivity of the sections stained with the preabsorbed YKL-40 antibody. The end feet layer (EFL) is barely visible in (B) and (F), and the presumed astroglial progenitors (arrow) in the subventricular zone (SVZ) in (C) is no longer positive following preabsorption (D). Note the reactivity associated with the blood vessel in (C) (arrow) and the lack of reactivity in (D) (arrow). (G) Quantitative real-time RT-PCR analysis of *YKL-40* mRNA expression in the human developing forebrain from tissue samples dissected from two human embryos (aged 6 weeks and 5 days post-conception and 7 wpc) at the 7th and 8th wpc and three human fetuses (aged 8 wpc, 8 weeks and 3 days post-conception, and 9 wpc) at the 9th and 10th wpc. Relative mRNA expression is shown (meninges=1). Only one meninges sample was available for analysis. A significant difference between average expression values obtained in the telencephalon (n=4) and the choroid plexus (n=3) was observed (indicated by *, Students t-test, p=0.029). Error bars represent one standard deviation. Scale bar: A–B: 200 µm, C–D: 50 µm, E–F: 200 µm. Same magnification in (A-B), (C-D) and (E-F).

RNA was isolated from the tissue sample using TRIzol Reagent (Invitrogen) and RNA quality was determined by agarose gel electrophoresis. cDNA was synthesized with SuperScript II (RNase H-) reverse transcriptase (Invitrogen) according to manufacturer's instructions. Real-time quantitative RT-PCR (QPCR) analysis was performed using an ABI 7500 Fast real-time PCR system and with a LightCyclerFastStart DNA MasterPLUS SYBR GreenI kit (Roche, Hvidovre, Denmark). All samples were analyzed in duplicates. Expression levels were determined using a standard curve, generated by 10-fold dilutions of the PCR product. Data were normalized using the average expression value of four housekeeping genes (*B2M, HPRT, ATP6A* and *COX4A*) and related to the choroid plexus at 6 weeks and 5 days post-conception, as we have shown previously a strong YKL-40 expression in developing human choroid plexus (Johansen et al. 2007). YKL-40 primer sequences were: 5' AATGGGTGTGAAGGCGTCT 3' and 5' GGTACAGA GGAAGCGGTCAA 3'. Primer sequences for the housekeeping genes are available upon request. Statistical analysis was performed using Student's *t*-test.

Results

Immunostaining for YKL-40 resulted in a clear and well-defined staining pattern, irrespective of the fixative used. Control sections, where the YKL-40 antibody was preabsorbed with YKL-40 antigen, showed a lack of or a strongly diminished reactivity at the early and late fetal ages (Fig. 1A-1F). QPCR was used to relate the YKL-40 distribution observed with immunohistochemistry at the protein level to its mRNA expression in the forebrains of embryos and fetuses at 7^{th}-10^{th} wpc. The telencephalic wall, meninges and choroid plexus from two human embryos at the 7^{th} and 8^{th} wpc (aged 6 weeks and 5 days post-conception and 7 wpc) and three human fetuses in 9^{th} and 10^{th} wpc (aged 8 wpc, 8 weeks and 3 days and 9 wpc) showed positive YKL-40 mRNA expression, with the strongest expression observed in the meninges (Fig. 1G). The choroid plexus showed significantly stronger expression than that in the telencephalon (Student's *t*-test, p=0.029).

The distribution of YKL-40 immunoreactivity is described in relation to the important developmental features of the human forebrain, and is based on and, in some cases, normalized against, gestational weeks or CRL to estimate the approximate number of wpc.

6^{th} week: Early neurogenesis (Bystron et al. 2008) and formation of radial glial cells (RGCs) (Howard et al. 2008), formation of the preplate (PP) (Bystron et al. 2008) and hippocampal thickening (Humphrey 1966).

7^{th} week: The choroid plexus of the lateral ventricles emerges (Jacobsen et al. 1982). Reelin-producing Cajal-Retzius cells (CRCs) (Abraham et al. 2004) and the subventricular zone (SVZ) appear (Møllgård and Jacobsen 1984; Bystron et al. 2008).

8^{th} week: Formation of the cortical plate (CP) (Bystron et al. 2008).

9^{th} to 11^{th} week: The intermediate zone (IZ) and subplate (SP) can be separated by different markers (Bystron et al. 2008) and microglia appear in the telencephalon (Rezaie et al. 2005).

12^{th} to 14^{th} week: S100-positive astrocytes appear in the fimbria and hippocampus (Janas et al. 1991), the subpial granular layer (SGL), containing CRCs, is formed (Gadisseaux et al. 1992; Meyer 2010) and the outer subventricular zone (OSVZ) can be distinguished (Hansen et al. 2010).

15^{th} to 21^{st} week: CRCs and SGL cells descend to a deeper position within the marginal zone (MZ) (Meyer 2010). The superficial part of the subpial glial end feet layer has not yet transformed into a subpial glia limitans, which occurs at 25^{th} to 28^{th} wpc (Kadhim et al. 1988).

YKL-40 Protein Distribution in 6^{th} to 8^{th} wpc Embryos

6^{th} wpc: Immunohistochemistry revealed a strong YKL-40 reaction in the rostral midline, with a clear gradient of decreasing staining away from the midline. The immunoreaction spanned the entire neuroepithelium but was strongest at the ventricular lining of the cerebrospinal fluid (CSF)-brain interface (CBI), in some neuroepithelial/RGCs of the ventricular zone (VZ) and cells of the developing PP (Fig. 2A). The remaining neuroepithelium in the forebrain showed staining corresponding to apico-basal processes. The choroid plexus and meninges are not yet formed, but the neural crest-derived leptomeningeal cells covering the early forebrain showed strong YKL-40 staining (arrowheads in Fig. 2A).

7^{th} wpc: The ventricular lining was YKL-40 immunoreactive in some areas of the forebrain, and the VZ corresponding to the cortico-choroid boundary was also immunopositive (Fig. 2B). Small YKL-40 reactive processes, similar to basal processes of neuroepithelial cells and/or end feet of RGCs, were distinctly lining the outer surface of the hem, with more diffuse immunoreactivity when moving through the hippocampal primordium. Similar YKL-40-immunopositive processes reaching the pial surface as triangular end feet formed a subpial layer in the outermost part of the PP in most of the neocortex in the forebrain. The lamina terminalis and the epithelium of the early developing choroid plexus of the lateral ventricles showed strong YKL-40 immunoreactivity by the end of the 7^{th} week. The pia-arachnoid could be clearly distinguished from the future dura, and leptomeningeal cells and some of the small vessels surrounding the brain displayed cytoplasmic immunostaining for YKL-40.

8^{th} wpc: As observed in the 7^{th} week, specimens the ventricular lining and the small processes lining the outer surface of the hem showed positive YKL-40 staining. The

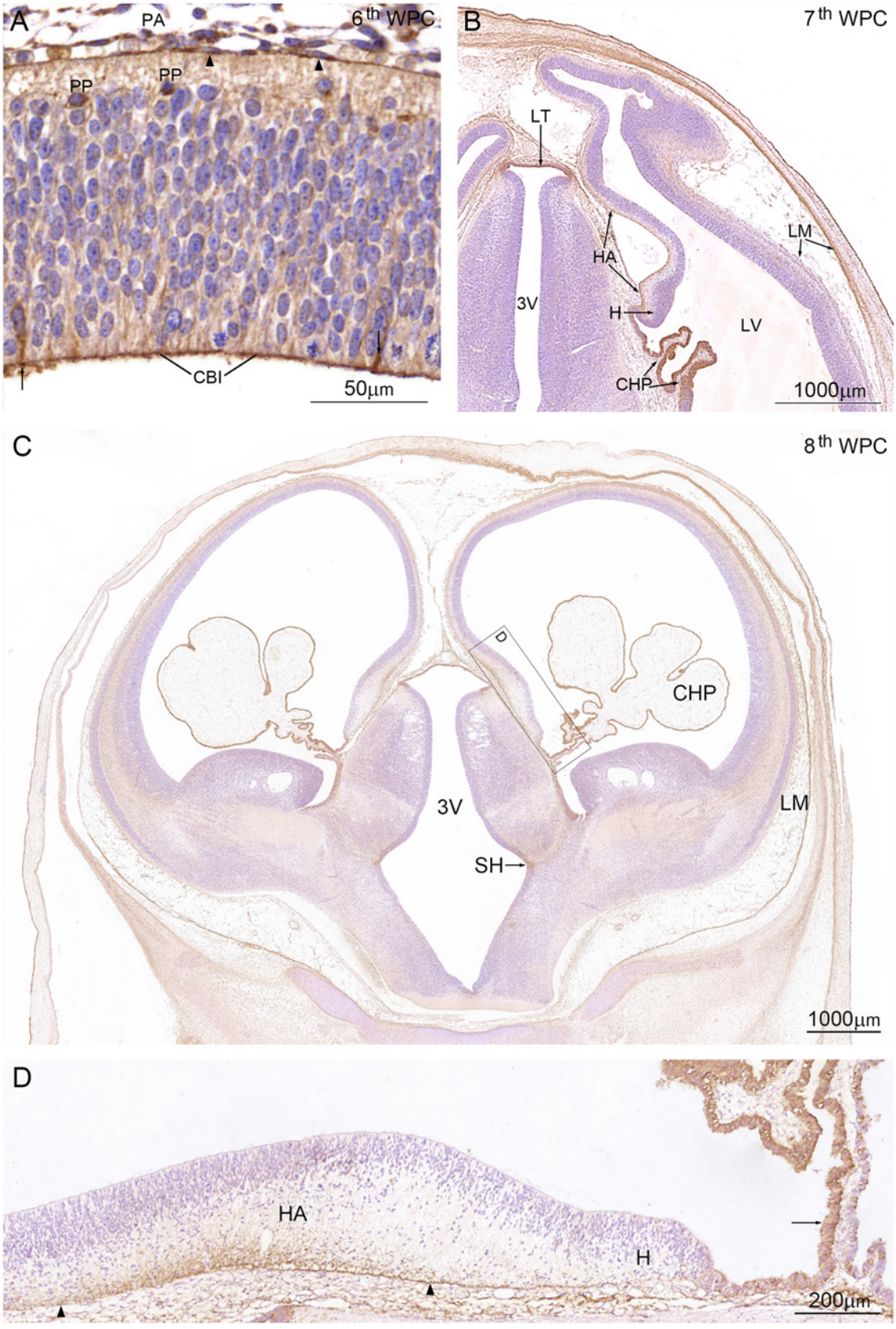
A
PA
6th WPC
PP
PP
CBI
50µm
B
7th WPC
LT
LM
HA
3V
H
LV
CHP
1000µm
C
8th WPC
D
CHP
3V
LM
SH
1000µm
D
HA
H
200µm

choroid plexus displayed a uniform, strong reactivity toward the end of the 8th wpc (Fig. 2C), and showed cytoplasmic staining in all of the distal glycogen-filled cells and a strong YKL-40 reactivity in the part of the root that is in direct continuity with the hem area and the hippocampal anlage (Fig. 2D). The subpial layer of possible radial glial end feet became increasingly immunoreactive during the 8th week, with the strongest reactivity corresponding to the outer surface of the hippocampal anlage and the lateral part of the dorso-lateral wall (Fig. 2C-2D). Leptomeningeal cells in the pia-arachnoid and many of the small vessels in the meninges showed a strong YKL-40 immunostaining.

YKL-40 Protein Distribution in 9th to 21st wpc Fetuses

9th to 13th wpc: Immunoreactivity at this age corresponded to basal radial glial processes creating a subpial layer and to the ventricular lining, the choroid plexus epithelium and the leptomeninges. As in the embryos, the VZ corresponding to the cortico-choroid boundary was also YKL-40 positive. At 10 wpc, the YKL-40 reactive layer of radial glial end feet, which, in earlier specimens, had marked the outer surface of the hem, took a more rostral position lining the hippocampal primordium. From the 12th wpc, there was a distinct stratification of YKL-40 immunoreactivity in the forebrain, with a strong staining of the pia-arachnoid on the outside of the telencephalic wall and of the choroid plexus inside the lateral ventricle (Fig. 3). Within the telencephalic wall, the IZ was stained from the subiculum to the dorsal neocortex. This reactivity was due to multiple, small YKL-40-positive dots close to the IZ blood vessels. The lack of reactivity of the IZ of the hippocampal anlage was paralleled by a marked staining of the subpial lining of the MZ (Fig. 3). The SVZ and VZ showed no staining at low magnification apart from the positively stained VZ covering the fimbria.

Cells within the CP, SP and inner SVZ showed no YKL-40 immunoreactivity and Iba1-positive subpopulations of cells, characterized by large ovoid cell bodies and few or no short processes (putative microglia), were not YKL-40 positive (not shown).

14th to 21st wpc: The strong YKL-40 immunoreactivity of the choroid plexus and leptomeninges and the lack of reactivity in the CP and SP persisted during forebrain development from 14th to 21st wpc. The stratified YKL-40 distribution in the telencephalic wall, seen at low magnification at earlier stages, became increasingly more distinct with further maturation. At the cellular level, there were obvious differences in the YKL-40 reactivity in the IZ (Figs. 4, 5), the SVZ (Figs. 6, 7), the MZ (Figs. 8, 9), and the hippocampus (Fig. 10).

YKL-40 immunodistribution in the dorsal telencephalon of 15th wpc human fetuses showed weak reactivity in the inner half of the cerebral wall, where small dots of YKL-40 immunostaining were most prominent in the IZ (Fig. 4A), corresponding to the findings at 12thwpc. The SVZ and VZ showed virtually no reactivity at this low magnification (Fig. 4B). At the cellular level, a fine granular staining was obviously associated with small blood vessels (arrows in Fig. 4C), but whether the reaction product was associated with endothelial cells and/or pericytes could not be distinguished. GFAP-positive astrocytic end feet were not present in the IZ (not shown). Using confocal microscopy, the majority of the microvessel endothelial cells (EC) in the IZ/OSVZ showed positive von Willebrand Factor (vWF, endothelial cell marker) immunostaining (Fig. 5B) but no immunoreactivity for YKL-40. However, directly adjacent to the endothelial cells were YKL-40-positive pericytes, which covered segments of the outer endothelial cell membranes (Fig. 5C). The merged images demonstrate the absence of co-localization of vWF and YKL-40 (Figs. 5D and 6).

In the ventral telencephalon, a unique population of YKL-40-positive cells appeared in the SVZ corresponding to the border of the lateral ganglionic eminence at 14 wpc. These small, rounded cells displayed dense, cytoplasmic YKL-40 immunoreactivity. This pattern was still present in frontal cortex at 20 wpc, and similar cells were found covering the entire SVZ in the visual cortex, indicating a

Figure 2. YKL-40 protein distribution in a coronal section from an embryo at the 6th wpc (crown-rump length (CRL): 7 mm). (A) Leptomeningeal cells (arrowheads) in the pia-arachnoid (PA) have strong YKL-40 immunoreactivity. Apical surfaces of neuroepithelial cells forming the CSF-brain interface (CBI) are outlined by YKL-40 immunoreactivity and some neuroepithelial cells/radial glial cells (arrows) and preplate cells (PP) are YKL-40 positive. (B) Coronal section from a 7th wpc human embryo (CRL: 20 mm). The YKL-40 positive outer surface of the hippocampal anlage (HA) is shown between the two arrows. Epithelial cells of the newly-formed lateral ventricular choroid plexus (CHP) have strong YKL-40 immunoreactivity. The cortico-choroid boundary between the hem (H) and the plexus is YKL-40 positive. Leptomeninges (LM), in particular, the continuous part of the arachnoid, show strong YKL-40 immunoreactivity. In the rostral part of third ventricle (3V) the lamina terminalis (LT) shows strong YKL-40 immunoreactivity. (C) Coronal section from a late 8th wpc human embryo (CRL: 31 mm). Note the distinct reactivity of the LM and CHP epithelium compared with that of the telencephalic wall, where only marginal and intermediate zones show a weak YKL-40 immunoreactivity. A prominent sulcus hypothalamicus (SH) is seen in 3V. The boxed area includes the hippocampal anlage (HA), the hem (H) and the root of the choroid plexus, and is shown in higher magnification in (D). End feet and the outer marginal zone of the developing CA1 to CA4 of the hippocampus (between the arrowheads) show strong YKL-40 immunoreactivity. The dentate primordium between the right arrowhead and the hem is only immunostained in the end feet region in contrast to the unstained hem, which extends to the choroid plexus where the part of the root (arrow) adjacent to the hem shows strong YKL-40 immunoreactivity. Scale bars: A: 50 μm; B-C: 1000 μm; D: 200 μm.

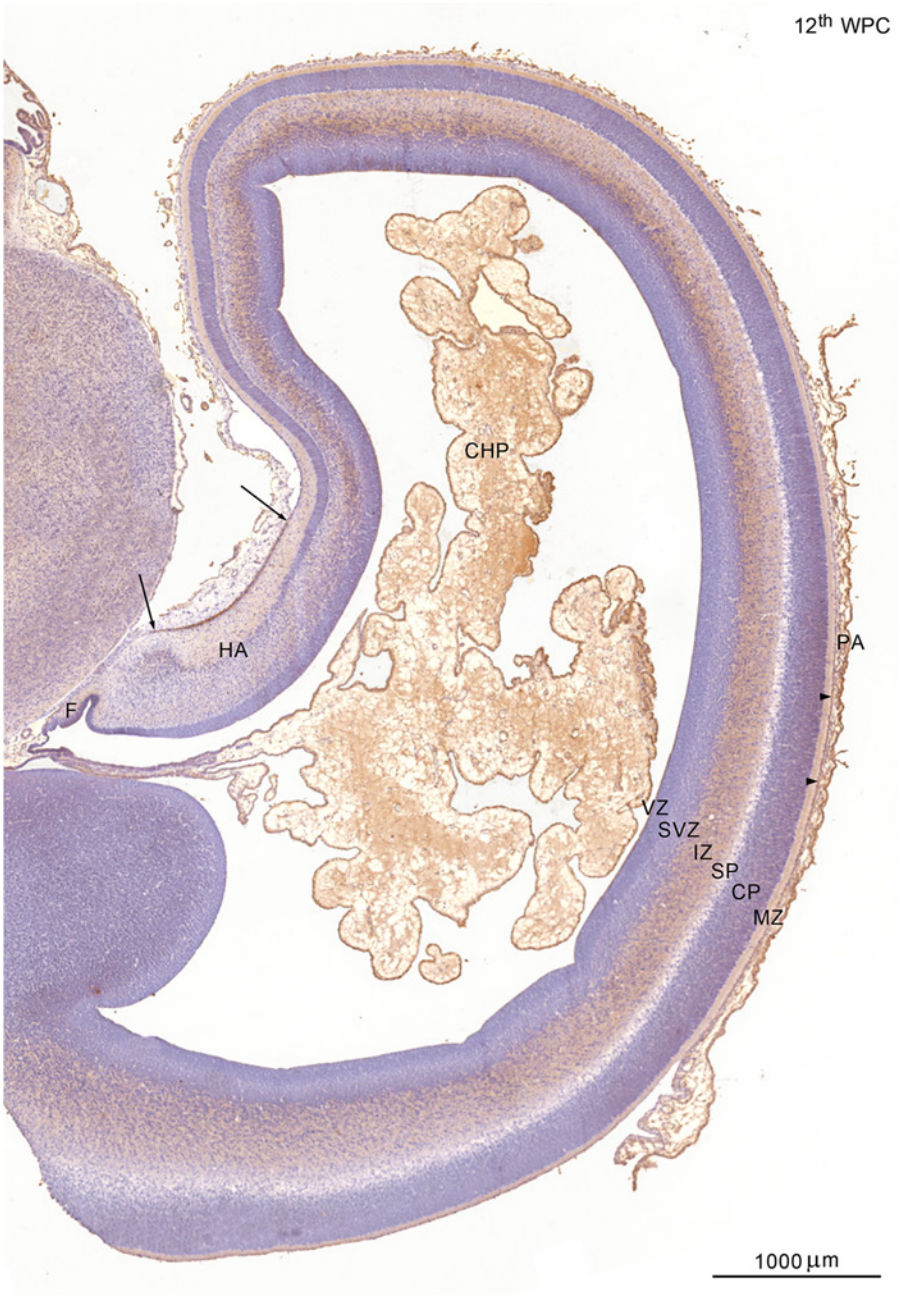

Figure 3. YKL-40 protein distribution in the neocortex and hippocampus of a 12th wpc fetus (crown-rump length: 75 mm). The pia-arachnoid (PA) immediately outside the telencephalic wall and of the choroid plexus (CHP) on the inside show strong YKL-40 immunoreactivity. Gradients within the wall include a marked staining of the outermost layer of the marginal zone (MZ) of the hippocampal anlage (HA) between the two arrows, and a consistent reactivity of the subpial line of the lateral neocortex (arrowheads). The cortical plate (CP) and subplate (SP) are not stained in contrast with the intermediate zone (IZ), which is strongly reacting from the subiculum via the medial (cingulate) cortex to the dorsal neocortex. The subventricular zone (SVZ) and ventricular zone (VZ) have no YKL-40 immunoreactivity at this low magnification except from the positively stained VZ covering the fimbria (F). Scale bar: 1000 µm.

Figure 4. YKL-40 protein distribution in the lateral parietal forebrain of a 15th wpc human fetus (crown-rump length: 111 mm). (A) The inner half of the cerebral wall has small dots of YKL-40 immunoreactivity in the intermediate zone (IZ), in contrast to the subventricular and ventricular zones (SVZ and VZ) which show virtually no YKL-40 immunoreactivity at this low magnification. (B) A higher magnification of the VZ–SVZ, with virtually no YKL-40 immunoreactivity. A small vessel with a YKL-40 positive endothelial cell/pericyte is seen in the lower part of the IZ (arrows). (C) Higher magnification of the IZ boxed area in (A). The fine granular staining of YKL-40 is associated with small blood vessels (arrows), but whether the reaction product is within endothelial cells and/or pericytes cannot be distinguished. A longitudinal vessel with patchy reactivity is seen (arrowheads). Astrocytes with end feet are not developed at this stage. Scale bars: A: 200 µm; B-C: 50 µm.

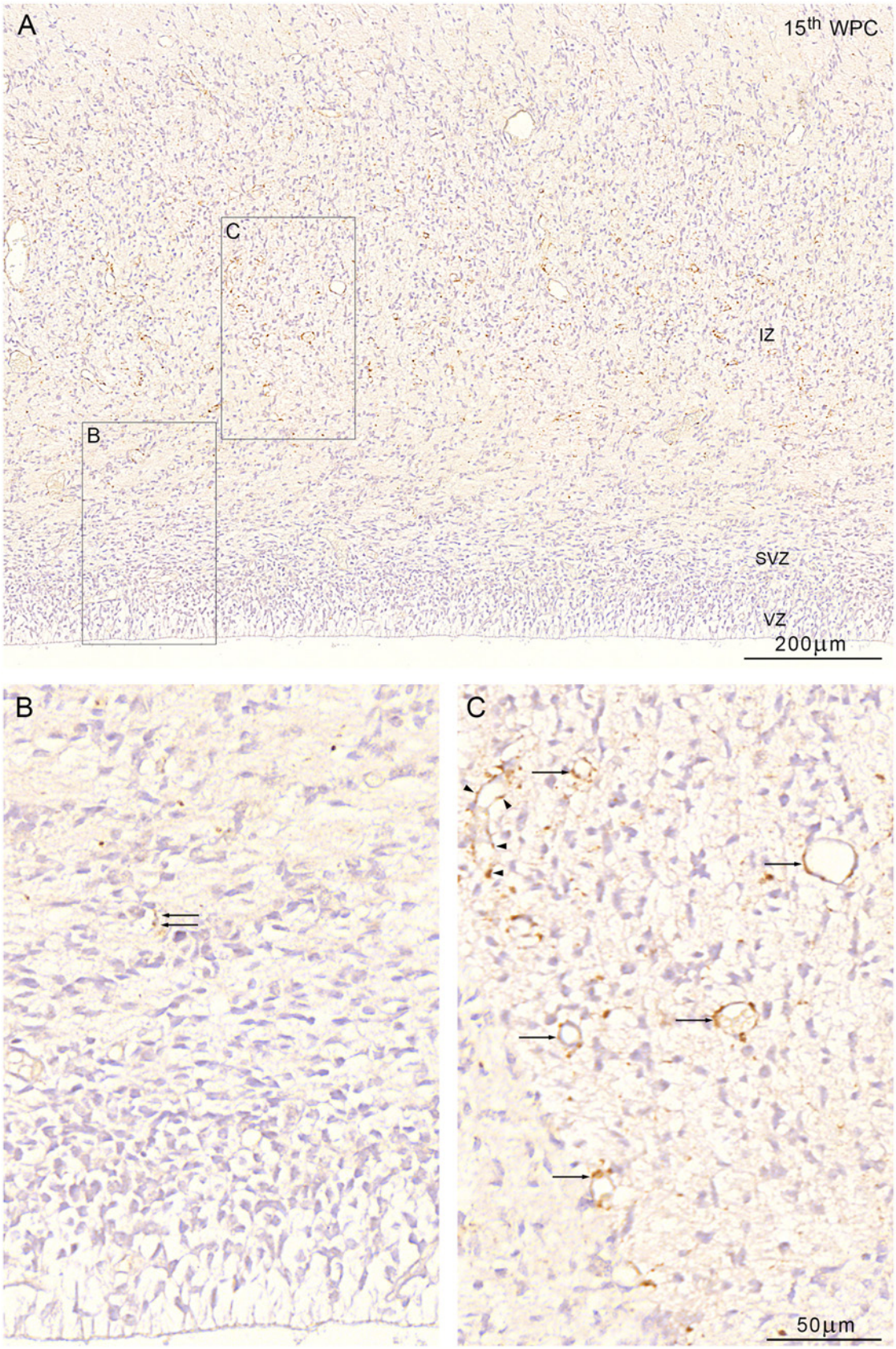
A
15th WPC
C
IZ
B
SVZ
VZ
200µm
B
C
50µm

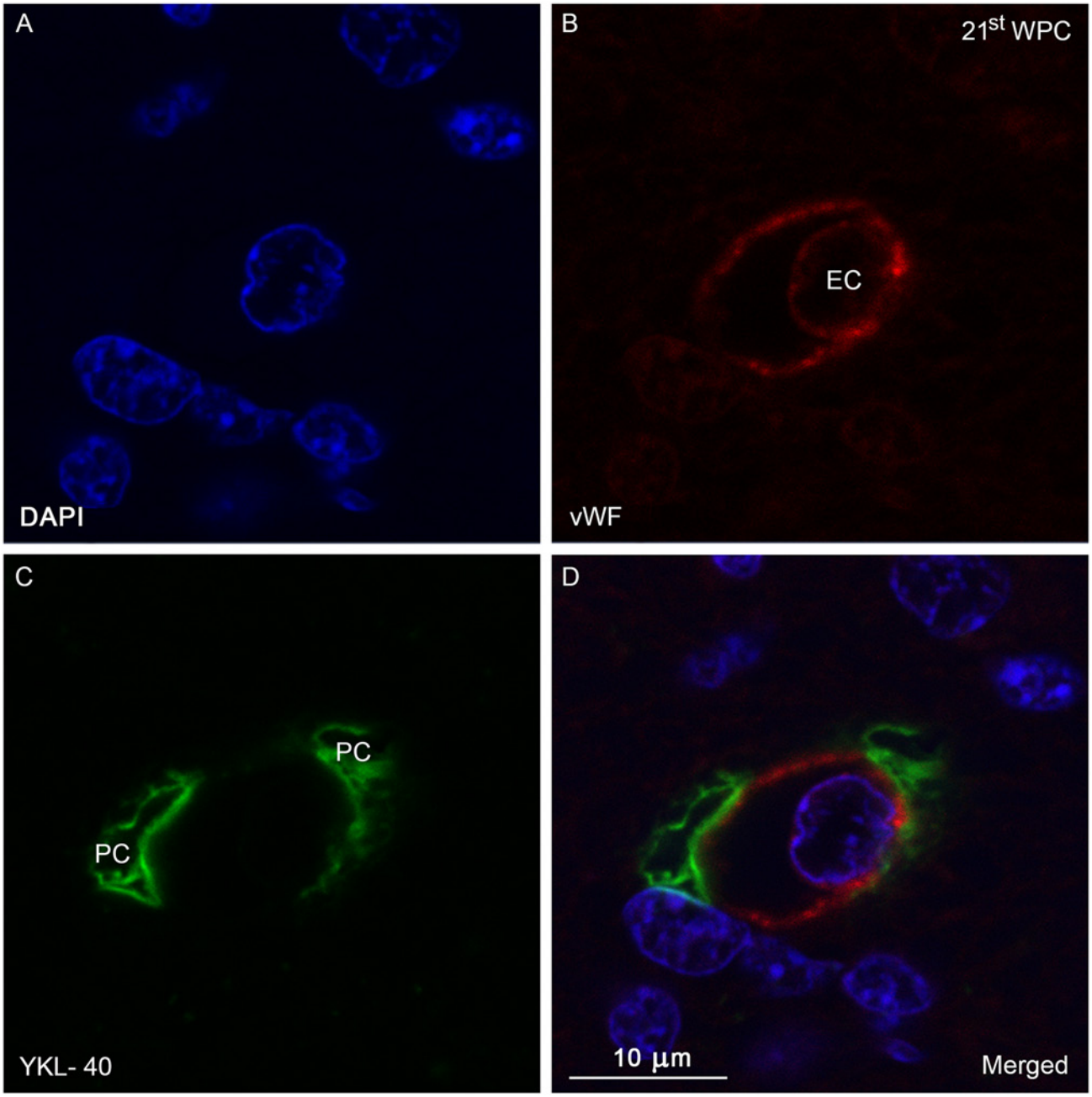

Figure 5. Confocal image of a double immunolabeled section of the occipital intermediate zone from a 21st wpc human fetus (crown-rump length: 200 mm) stained with antibodies against YKL-40 (green) and von Willebrand Factor (vWF; red) and nuclear counterstained with DAPI (blue). (A-D) Microvessel with an endothelial cell (EC) and surrounding pericytes (PC). (B) vWF-positive endothelial lining of an intermediate zone capillary and the EC. (C) Discontinuity of the surrounding YKL-40-positive PC. (D) Merged image showing the lack of co-localization of vWF and YKL-40 in the YKL-40-positive PC membrane adjacent to the endothelial lining. Scale bar: 10 µm.

differential spatio-temporal distribution of these YKL-40-positive cells. In a few segments of the VZ, for example, in the developing frontal and visual cortices, similar strongly reactive YKL-40-positive cells were observed. These cells were different from the earlier described pericytes in terms of both morphology and staining characteristics and never showed direct contact with the endothelial cells, as demonstrated by confocal microscopy and double immunolabeling with antibodies against YKL-40 and vWF in subventricular zone of the visual cortex (Fig. 6). The nuclei of the YKL-40-positive, rounded cells were larger than those of the pericytes. In order to elucidate whether these cells were

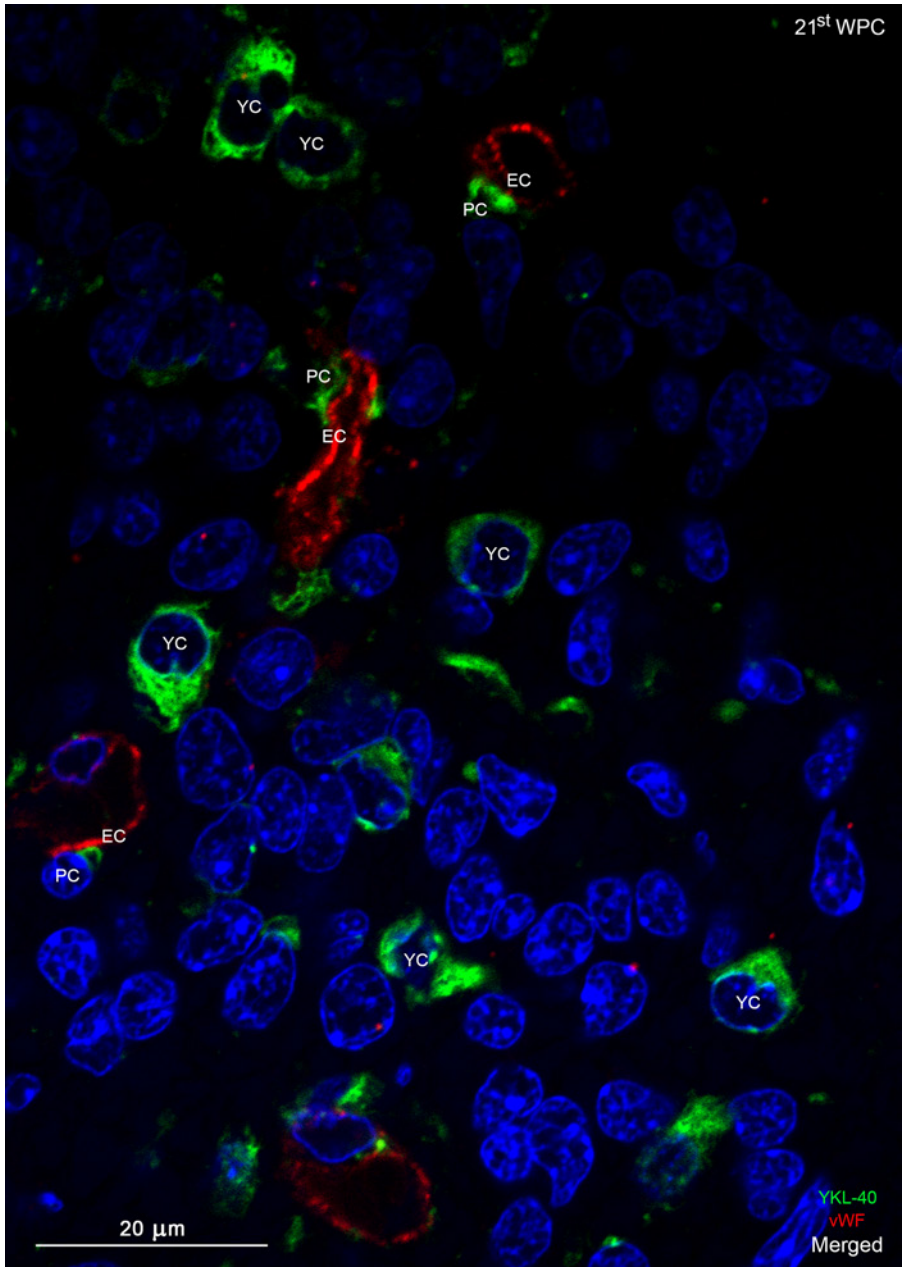

Figure 6. Confocal image of a double immunolabeled section of the occipital subventricular zone from a 21st wpc human fetus (crown-rump length: 200 mm) stained with antibodies against YKL-40 (green) and von Willebrand Factor (vWF; red) and nuclear counterstained with DAPI (blue). The YKL-40-immunopositive pericytes (PC) in the subventricular zone show a circumventing discontinuity of the vWF-immunopositive endothelial cells (EC) of the microvessels. YKL-40 immunoreactivity is found in small rounded cells (YKL-40-positice cells, YC) with a strong cytoplasmic staining surrounding the nucleus. These cells have no contact with microvessels. Scale bar: 20 µm.

GFAP-positive radial glial cells, sections were double immunolabeled with antibodies against YKL-40 and GFAP. Small clusters of YKL-40-immunopositive cells were closely associated with GFAP-positive radial glial fibers (RGF) and, in a few cases, co-localization was definitely observed (Fig. 7A-7D).

The outermost part of the MZ appeared as a YKL-40-immunopositive indented layer, with a staining reaction of varying intensity. As seen at earlier stages, there was a gradient of staining, with the strongest reactivity corresponding to the outer surface of the hippocampus, in particular the fimbria, and the lateral part of the dorso-lateral telencephalic wall. At the cellular level, a continuous layer of small YKL-40-reactive processes, corresponding to the end feet of radial glial cells, reached the pial surface as semicircular or triangularly stained elements (Fig. 8A). Only a few processes in the end feet layer were positive for GFAP (Fig. 8B). Large Cajal-Retzius cells and the transient population of subpial granular cells were YKL-40-negative (Fig. 8A). Confocal microscopy using double immunolabeling with antibodies against YKL-40 and GFAP showed strong

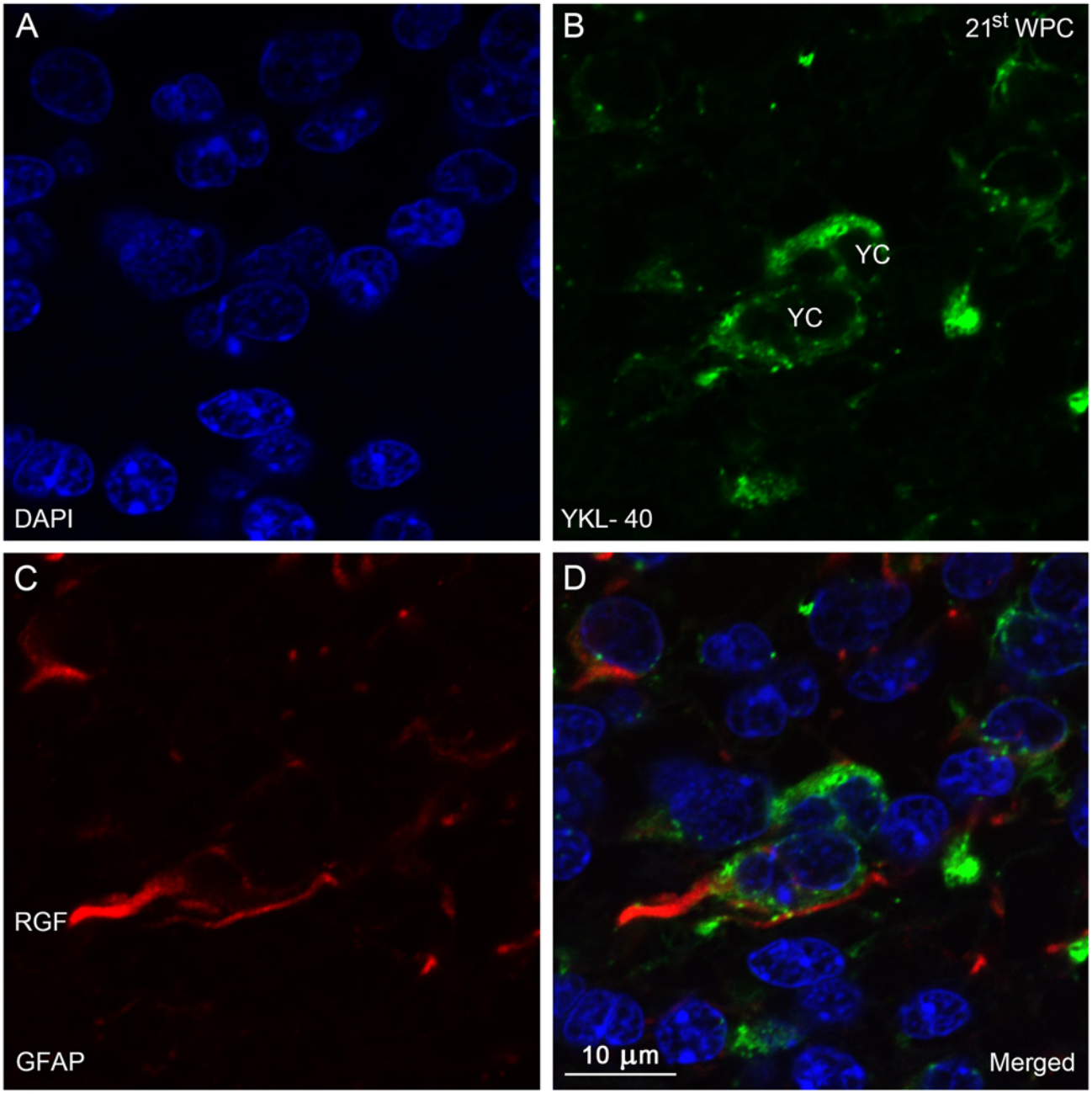

Figure 7. Distribution of YKL-40 and GFAP in the occipital subventricular zone from a 21st wpc human fetus (crown-rump length: 200 mm). Sections were stained with antibodies against YKL-40 (green) and glial fibrillary acidic protein (GFAP, red), counterstained with DAPI (blue) and examined in the confocal microscope throughout the z-axis. (A) DAPI. (B) YKL-40-immunopositive small rounded cells (YC). (C) GFAP-immunopositive radial glial fibers (RGF). In (D), note the co-localization between the GFAP-positive RGF and YKL-40. Several GFAP-positive YCs are seen with a strong cytoplasmic YKL-40 reactivity. Scale bar: 10 µm.

YKL-40 immunoreactivity (Fig. 8D) but virtually no GFAP staining (Fig. 8E) in the end feet layer (Fig. 8C). At higher magnification, the end feet layer was characterized by distinct YKL-40 staining, which seemed to be associated with the membranes of all end feet (Fig. 9). There was a marked decrease in the immunoreactivity closer toward the cortical plate. The YKL-40-immunostained leptomeningeal cells in the pia were

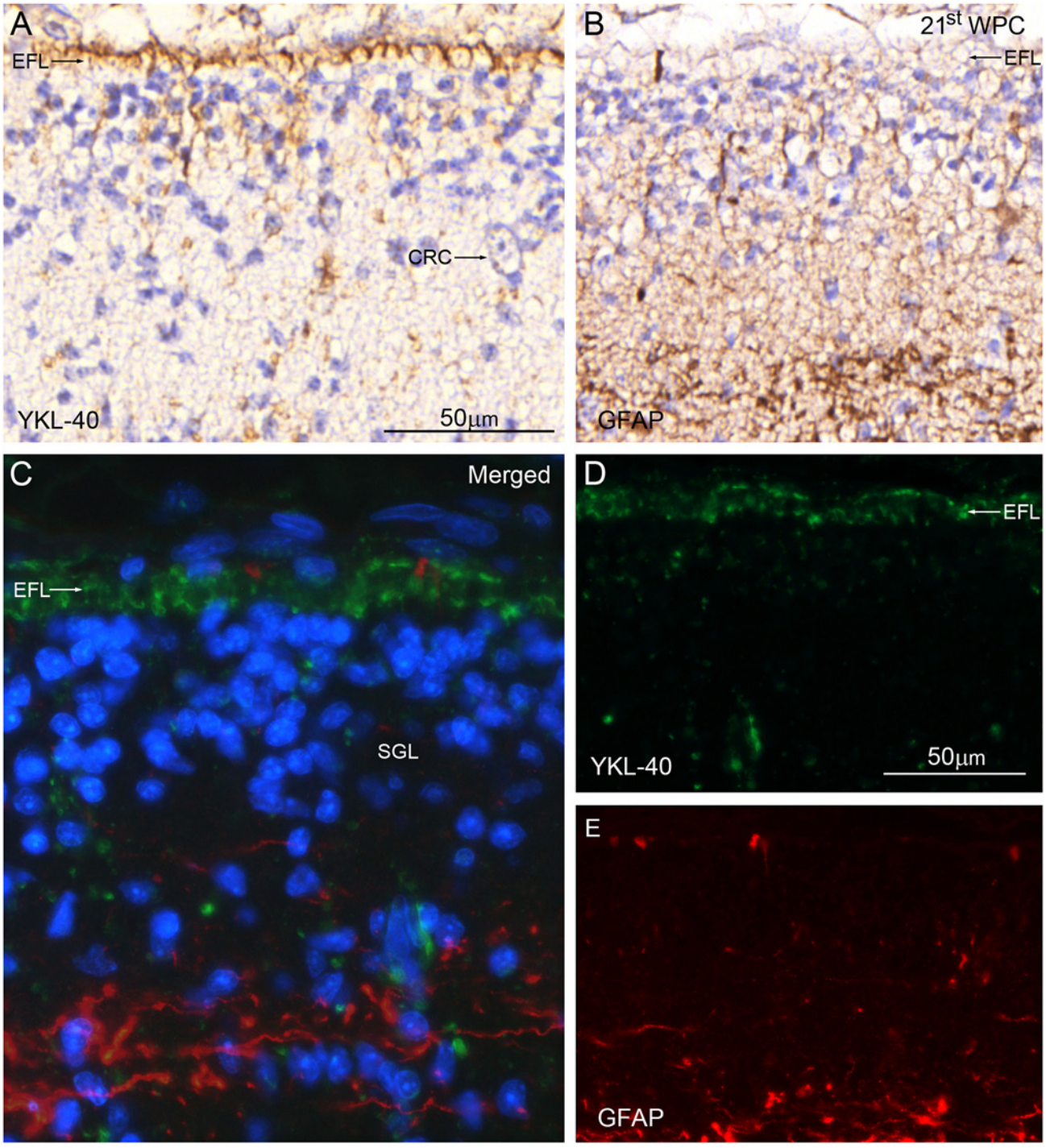

Figure 8. Distribution of YKL-40 and GFAP in the marginal zone from the dorso-lateral parietal cortex of a 21st wpc human fetus (crown-rump length: 200 mm). Consecutive sections are stained with antibodies against YKL-40 and glial fibrillary acidic protein (GFAP), nuclear counterstained with hematoxylin (A, B) or DAPI (C) and viewed with ordinary light microscopy (A-B) or confocal microscopy (C-E). In (A) and (D) the end feet layer (EFL) shows strong YKL-40 immunoreactivity; however, virtually no GFAP staining is seen in the EFL in (B) and (E). The large Cajal-Retzius cell (CRC) in (A) has no YKL-40 immunoreactivity. The marginal zone contains a transient population of YKL-40-negative cells corresponding to the subpial granular layer (SGL) shown with DAPI staining in the merged image in (C). Scale bars: A-E: 50 μm; the same magnification was used in (A-B), and in (C-E).

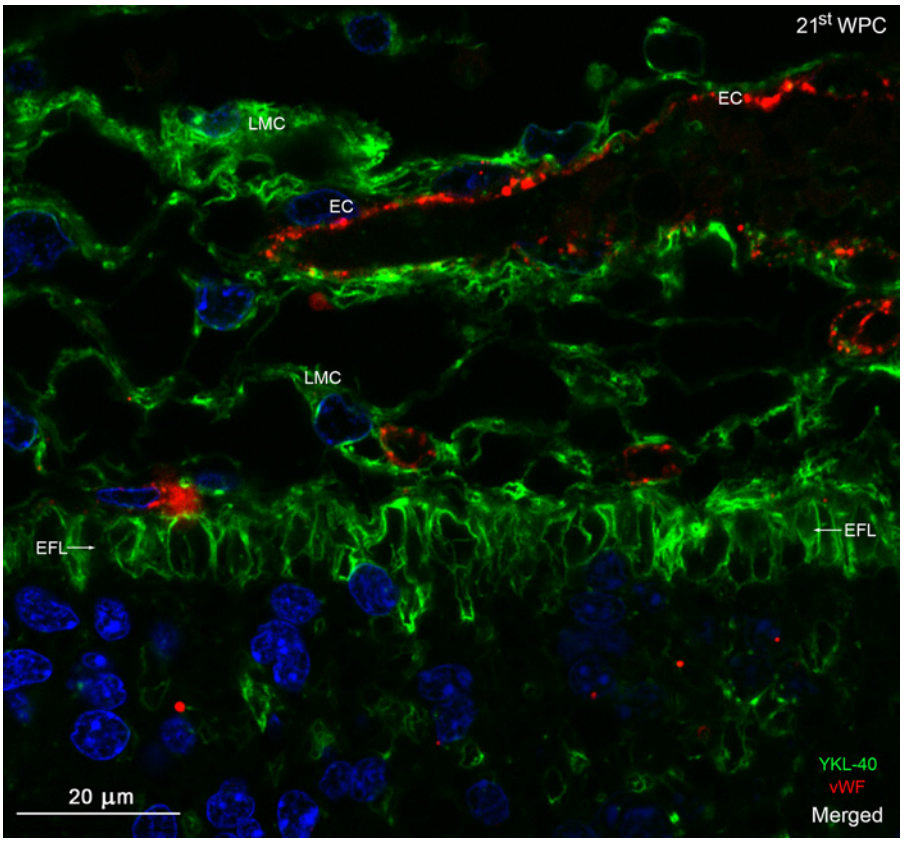

Figure 9. Distribution of YKL-40 and von Willebrand factor in the occipital marginal zone from a 21st wpc human fetus (crown-rump length: 200 mm). The section was stained with antibodies against YKL-40 (green) and von Willebrand Factor (vWF) (red), nuclear counterstained with DAPI (blue) and viewed using confocal microscopy. The YKL-40-immunopositive end feet layer (EFL, arrows) separates the leptomeninges and underlying marginal zone. No blood vessels penetrate the marginal zone in this section. Note the strongly immunoreactive leptomeningeal cells (LMC), some of which surround the vWF-positive endothelial cells (EC) of the vessels of the pia-arachnoid. The EFL forming the outermost part of the marginal zone shows a strong membranous reactivity, with a decreasing immunoreactivity within its deeper strata. Scale bar: 20 µm.

closely opposed to the end feet layer, whereas endothelial cells of the microvasculature of the pia were not positive for YKL-40 (Fig. 9).

The earlier described YKL-40-immunopositive features of the hippocampus, including the marked staining of the subpial layer of the marginal zone of subiculum, were much more pronounced at the later stages of development. Morphologically obvious astrocytes in the fimbria, a neuron-free region, showed a stronger YKL-40 immunoreactivity during the later half of the investigated time interval. Furthermore, a thin layer of YKL-40-positive cells, with several vertical and horizontal processes, separated the VZ from the future alveus (Fig. 10A). At the cellular level, a few YKL-40-positive pericytes were present and numerous strongly YKL-40-stained astrocyte-resembling cells formed a dense network, with many processes extending to the endothelial cells of the microvasculature in fimbria (Fig. 10B).

Discussion

Our study demonstrates a novel characterization of YKL-40 in the developing human forebrain. We show a marked YKL-40 immunoreactivity in neuroepithelial cells, some PP cells, radial glial end feet, leptomeninges and choroid plexus epithelial cells during the early stages of development. Later developmental features include an increasing number of YKL-40-immunopositive pericytes, particularly in the IZ and SVZ, and a population of small, rounded, YKL-40-positive cells in close relation to and occasionally overlapping with GFAP-positive radial glial fibers in the SVZ. The choroid plexus and the layer of radial glial end feet and its covering pia-arachnoid membrane are strongly YKL-40-immunopositive, and the astrocyte-resembling cells observed in the developing hippocampus are strongly reactive.

We detected the synthesis of *YKL-40* mRNA in the meninges, telencephalon and the choroid plexus. qRT-PCR analysis suggested stronger expression in the latter compared with that of the cerebral wall. However, this result should be interpreted with some caution because of the low number of samples available for analysis. The delicate membranous staining of the entire subpial glial end feet layer, as determined by confocal microscopy, is compatible with an uptake of YKL-40.

We suggest that YKL-40 plays a role in the developing brain barriers and that the YKL-40-positive, small, rounded cells are astroglial progenitors possibly involved in the differentiation of a particular astrocytic lineage. Furthermore, we propose that the glial progenitors, leptomeninges, choroid plexus epithelium, pericytes and, later, a subpopulation of astrocytes are the YKL-40-producing elements in the developing human forebrain.

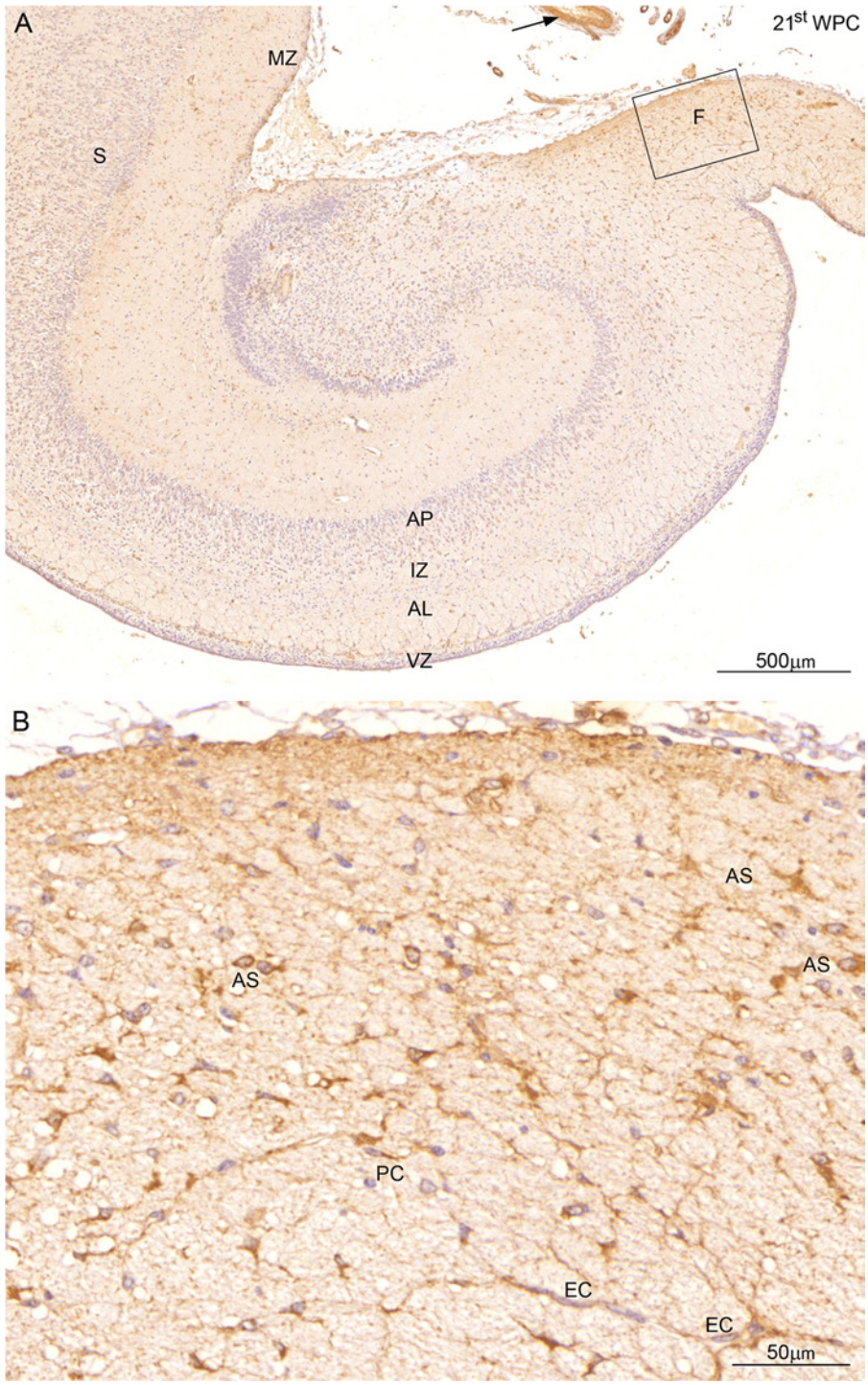

Figure 10. Distribution of YKL-40 in a coronal section of the hippocampus from a 21st wpc human fetus (crown-rump length: 200 mm). (A) In contrast to the weak staining of the hippocampus, the fimbria (F)—shown at higher magnification in (B)—and smooth muscle cells (arrow) in blood vessels in the subarachnoid space show strong YKL-40 immunoreactivity. The subpial layer of the marginal zone (MZ) of the subiculum (S) and the cellular layer between alveus (AL) and the ventricular zone (VZ) are also reactive. The intermediate zone (IZ) facing the ammonic plate (AP) shows very small dots of YKL-40 immunoreactivity. In (B), which is a larger magnification of the boxed area in (A), many YKL-40-immunopositive astrocyte-resembling cells (AS) form a network with endothelial cells (EC) and pericytes (PC). Scale bars: A: 500 µm; B: 50 µm.

The Brain Barrier System and Early Angiogenesis

In the 5th to 6th wpc, prior to vascularization of the forebrain anlage and choroid plexus development, a dense vascular plexus dominates the developing subarachnoid space between the inside of the differentiating membranous bones of the calvarium and the pial covering of the forebrain surface. After the penetration of the first vessels into the telencephalic wall and the appearance of the choroid plexus, the following mesenchymal/neuroectodermal interfaces comprise the initial brain barrier system: 1) The blood-brain barrier (BBB) proper across the YKL-40-immunonegative cerebral endothelial cells, surrounded by YKL-40-positive pericytes with a differential immunoreaction; 2) the blood-CSF barrier at the strongly YKL-40-positive choroid plexus epithelium; and 3) the blood-arachnoid and

pia-brain surface barriers, with strongly YKL-40-positive leptomeningeal cells and subpial radial glial end feet. In addition, within the neuroectoderm, per se, 4) there is a barrier interface between the CSF and the brain interstitial fluid at the apical neuroepithelial membrane (Saunders et al. 2008) lined by dense YKL-40 immunoreactivity in the early brain.

An important interface in the early steps of the brain barrier development is the blood-CSF barrier (Stolp et al. 2013) where we found strong *YKL-40* mRNA expression in the choroid plexus. Prominent YKL-40 staining was evident as early as 7 wpc (49 dpc) when the choroid plexus of the lateral ventricles first appears in the human embryonic brain. This is in accordance with previously described *YKL-40* mRNA expression findings (Johansen et al. 2007). Our results suggest that YKL-40 is produced by the choroid plexus epithelium and secreted into the ventricular system.

A variety of secreted diffusible factors from fetal meninges regulate neural migration and positioning and organize the pial basement membrane, which is a critical anchor point for the radially oriented fibers of neuroepithelial stem cells (Siegenthaler and Pleasure 2011). Signaling molecules identified so far include the chemokine SDF-1, BMP7 and the morphogen all-trans retinoic acid (atRA), which seem to be involved in the decision of neuroepithelial cells to generate neurons and intermediate progenitor cells destined for the SVZ via communications with adjacent radial glial end feet (Siegenthaler et al. 2009). We suggest that YKL-40 can be added to the list of secreted diffusible factors, as the meninges both show profound *YKL-40* mRNA and protein expression and subpial radial glial end feet are YKL-40 immunoreactive. Thus, the pronounced YKL-40 immunoreactivity of the entire end feet layer associated with its bulging/curling membranes is best accounted for by receptor-mediated uptake of YKL-40 produced by leptomeningeal cells from the subarachnoid space.

Early in brain development, at the CSF-brain interface lining the cerebral ventricles, the cells of the neuroepithelium are linked by strap junctions (Møllgård and Saunders 1986; Møllgård et al. 1987), which offer an effective limitation to intercellular diffusion, at least for large molecules (Fossan et al. 1985). This barrier interface is lined by dense YKL-40 immunoreactivity apparently associated with apical neuroepithelial membranes and thus compatible with receptor-mediated uptake.

Pericytes are required for blood-brain barrier integrity during embryonic angiogenesis following an initial neural progenitor induction of endothelial cells to express blood-brain barrier specific proteins, including tight junction molecules and specific nutrient transporters (Daneman et al. 2010). Pericytes then strengthen the endothelial barrier during further embryogenesis by regulating tight junction structure, limiting the rate of transcytosis, and inhibiting the expression of leukocyte adhesion molecules. Only later the astrocytic processes are developed, and surround the endothelial and pericytic membranes, supporting the blood-brain barrier functionality (Daneman et al. 2010). Establishment, maintenance and repair of the endothelial barrier depend on pericytes and astrocytes, and both cell types are linked to BBB disruption in disease (Argaw et al. 2012). Early angiogenesis also depends on pericyte functionality, as migrating angiogenic pericytes precede and guide the endothelial cells of the growing telencephalic microvessels (Virgintino et al. 2007).

The role of YKL-40 as an angiogenic factor has been studied by Francescone et al. (2011) in a human brain tumor cell line, and they showed that vascular endothelial growth factor (VEGF), a primary angiogenic promoter, is up-regulated by YKL-40. Further, their results showed that not transient but long-term inhibition of VEGF induced the expression of YKL-40, indicating that VEGF does not regulate YKL-40 but long-term inhibition of VEGF may induce YKL-40 as an angiogenic compensative response (angiogenic rebound), providing evidence for YKL-40 as a tumor maintaining angiogenic factor (Francescone et al. 2011; Shao 2013). We found YKL-40-positive pericytes in the microvasculature of both pial and periventricular vessels, but the staining reaction differed between regions and stages. This indicates that YKL-40 has a function both in the BBB proper and in angiogenesis, as described earlier. Within the telencephalic wall, YKL-40 appears associated with the developing vascular system, particularly in the portion of the vasculature that traverses the SVZ and IZ corresponding to the ascending arterial network (Vasudevan et al. 2008).

The passage of immune cells through the brain barriers to the CNS is a complex process, but an essential aspect in neuroinflammation and of normal function, both during development (e.g., microglia, which are of myeloid origin) and later in life (reviewed by Stolp et al. 2013). Using an in vitro BBB model, Correale and Fiol (2010) showed that YKL-40 significantly facilitates migration of peripheral blood mononuclear cells across the BBB. We propose that the observed YKL-40 expression associated with the developing brain barrier system is involved in controlling local angiogenesis and access of peripheral cells to the forebrain via YKL-40 secretion from choroid plexus epithelium, leptomeningeal cells and pericytes.

Microglia

Blood monocytes are known to enter the early human forebrain via choroid plexus and meninges to become amoeboid microglial cells (Aguzzi et al. 2013). Early colonization is initially restricted to the IZ. A second wave of monocytes penetrates into the brain via the vascular route at about 12 wpc and remains confined to the IZ/white matter (Verney et al. 2010). Areas known to harbor microglia are the inner

SVZ, SP, lower cortical plate and restricted laminar bands at the axonal crossroads in the white matter (Rezaie et al. 2005; Verney et al. 2010; Cunningham et al. 2013). Studies indicate that microglia do not show YKL-40 staining in vivo (Bonneh-Barkay et al. 2010; Craig-Schapiro et al. 2010). In the present study, cells with microglial characteristics were not YKL-40-immunopositive within telencephalic parenchyma in 10th wpc and later fetuses, in support of the previous findings (Bonneh-Barkay et al. 2010).

Neuroepithelial Cells, Radial Glial Cells and Astroglial Progenitors

In the early embryonic period, the pros- and early telencephalic wall only consist of neuroepithelial cells. At the beginning of neurogenesis, neuroepithelial cells transform through asymmetric divisions into radial glial cells (RGCs) (Götz and Huttner 2005; Howard et al. 2008). Ovoid RGC nuclei are situated in the VZ and SVZ of the developing neocortex and in the VZ of the hippocampus. The basal end feet of these bipolar cells face the pial surface of the fetal cerebrum (Bystron et al. 2008; Howard et al. 2008), and shorter apical processes form the ventricular surface (Pinto and Götz 2007; Howard et al. 2008). The RGCs may be regarded as neural stem cells. In the neocortex, the majority of RGCs initially generate neurons, which migrate along the radial glial fibers to their final destination in the cortex and, as corticogenesis progresses, they concurrently give rise to glial lineages (Malatesta et al. 2000; Pinto and Götz 2007). In the adult subependymal zone and subgranular zone (in rodents), a population of neural stem cells with astrocyte-like morphology and marker expression persists as descendants of RGCs (Alvarez-Buylla et al. 2002; Bonfanti and Peretto 2007; Howard et al. 2008). Recent studies have shown that astrocytes are heterogeneous in developmental origin, genetic profiling and function both in normal development and disease (Zhang and Barres 2010; García-Marqués and López-Mascaraque 2013). A very recent analysis of the clonal dispersion of astrocytes in the mouse cerebral cortex indicates that heterogeneous astroglial populations arise from specialized progenitor cells (García-Marqués and López-Mascaraque 2013).

In this study, the neuroepithelium of 6th wpc embryos was YKL-40-positive with cytoplasmic staining and demonstrated a gradient with a strong reactivity confined to the midline corresponding to the distribution of a subset of SSEA (stage-specific embryonic antige)4-positive neuroepithelial and early radial glial cells; this was also shown previously in the same material (Barraud et al. 2007). Although subtle, the cytoplasmic YKL-40 staining spanned the entire VZ, with processes into the PP and increased reactivity in the outermost part of the PP, suggesting that YKL-40 is expressed by neuroepithelial cells/radial glial cells (neural stem cells) in the early VZ. At later stages, radial glial cells of the VZ were not YKL-40-immunopositive, though we consistently found YKL-40 reactivity in possible RGC end feet, as described earlier. A proof of whether the neuroepithelium of the forebrain wall, including some morphogenetic centers, synthesizes or takes up YKL-40 will require in situ hybridization studies and a demonstration of a receptor for YKL-40.

We observed strongly YKL-40-positive PP cells prior to the appearance of the cortical plate. This could be due to uptake via apical PP cell processes, which terminate on the pia-arachnoid membrane, the cellular elements of which showed marked *YKL-40* mRNA and protein expression. No cellular elements corresponding to the cortical plate, reelin-producing Cajal-Retzius cells in the MZ (Abraham et al. 2004), or to GABAergic inhibitory interneurons migrating tangentially primarily within the SVZ (Hansen et al. 2013) showed YKL-40 immunoreactivity either in 7th week or later. The development of the subpial granular layer in 12th–14th wpc (Gadisseaux et al. 1992) was not reflected by a parallel appearance of numerous small YKL-40-positive cells in the MZ. From 14 wpc, we found a population of small, rounded, strongly YKL-40-positive cells in the SVZ with a differential spatio-temporal distribution. At 20 wpc, these cells were closely aligned to GFAP-positive radial glial fibers and, in a few cases, co-expression was evident, indicating that a fraction of GFAP-positive RGCs are YKL-40-immunoreactive whereas a larger subset migrate along the RGF in the SVZ.

Based on our findings of YKL-40-positive astrocyte-resembling cells in the developing fimbria, a neuron-free region and lack of YKL-40 reactivity in neuron forming regions mentioned above, we suggest that the YKL-40-positive cells in the SVZ represent a subpopulation of astroglial progenitors. As earlier described, YKL-40 reactivity is observed in relation to the brain barrier system, e.g., in RGC end feet, but we do not yet know if the possible astroglial progenitors described in this paper are more specifically involved in a general barrier function. Whether these cells contribute to the population of adult human neural stem cells in the subependymal zone is unknown. Further on-going studies are necessary to characterize this intriguing population of YKL-40-positive cells and confirm their lineage potential.

Clinical Aspects

Due to the presence of the brain barrier system and the muted inflammatory response within the brain parenchyma, the brain has been considered to be an immune privileged site. However, it is now suggested that neuroinflammation plays an important role in almost all neurological disorders and that the brain barrier system can contribute to this through either normal immune signaling and a maintained capacity for immune-surveillance of the brain, or via

disruption of various structural and functional components of the barrier system (for recent review, see Stolp et al. 2013). Inflammation-induced changes in the brain barrier system during development may contribute to serious developmental disorders, or change the susceptibility of the brain to later onset conditions, such as schizophrenia and neurodegenerative disease (Stolp et al. 2013). A role of YKL-40 in inflammation and immune responses could be explained by a general YKL-40-related participation in barrier function.

Glioblastoma multiforme is a common, heterogeneous and very aggressive malignant primary brain tumor. The origin of glioblastomas is still not fully grasped, but studies imply that a minor population of cancer stem cells maintain and may initiate the tumor (Singh et al. 2003; Park and Rich 2009;Schiffer et al. 2010). *YKL-40* mRNA and YKL-40 protein expression are higher in glioblastoma than in astrocytic and oligodendroglial tumors, increase with glioma grade and high *YKL-40* expression is associated with poor response to radiation and short time to disease progression and death (Pelloski et al. 2005; Colin et al. 2006; Rousseau et al. 2006; Iwamoto et al. 2011). Rousseau and co-workers (2006) found YKL-40 immunoreactive blood vessels in glioma tissue and YKL-40-expressing tumor cells were preferentially located in the close vicinity of blood vessels. They speculate that the increasing YKL-40 expression between low to high grade astrocytomas supports the involvement of YKL-40 in angiogenesis (Rousseau et al. 2006). The YKL-40-positive astroglial progenitor cells, together with previously described local YKL-40 secreting pericytes found in this study, form a new interesting possible background for glioblastomas.

In summary, our results suggest that the prominent YKL-40 expression, which is associated with the brain barrier system in the developing human brain, is involved in controlling access of peripheral cells to the forebrain and a segmental CNS angiogenesis via YKL-40 secretion from pericytes, choroid plexus epithelium and leptomeninges. Furthermore, YKL-40 immunoreactivity is present in a subpopulation of possible astroglial progenitor cells migrating along radial glial fibers in the SVZ. We suggest that YKL-40 could be involved in their switch into a particular astrocytic lineage. Future on-going studies are necessary to confirm their lineage potential and their possible role in glioblastomas and to elucidate the contribution of YKL-40 to a general barrier function involved in neuroinflammation.

Acknowledgments

We thank S. Forchhammer, H. Hadberg, P. S. Froh and K. Ottosen, Department of Cellular and Molecular Medicine, Faculty of Health and Medical Sciences, University of Copenhagen, Copenhagen, Denmark for excellent technical assistance. We thank Professor Paul A Price, Department of Biology, University of California, San Diego, USA, for providing the YKL-40 antibody.

Declaration of Conflicting Interests

The author(s) declared no potential conflicts of interest with respect to the research, authorship, and/or publication of this article.

Funding

The author(s) disclosed receipt of the following financial support for the research, authorship, and/or publication of this article: This work was supported by the Vera and Carl Johan Michaelsen Foundation [grant number 34077 to K.M.].

References

Abraham H, Pérez-García CG, Meyer G (2004). P73 and Reelin in Cajal-Retzius Cells of the Developing Human Hippocampal Formation. Cereb Cortex 14:484-495.

Aguzzi A, Barres BA, Bennett ML (2013). Microglia: scapegoat, saboteur, or something else? Science 339:156-161.

Alvarez-Buylla A, Seri B, Doetsch F (2002). Identification of neural stem cells in the adult vertebrate brain. Brain Res Bull 57:751-758.

Argaw AT, Asp L, Zhang J, Navrazhina K, Pham T, Mariani JN, Mahase S, Dutta DJ, Seto J, Kramer EG, Ferrara N, Sofroniew MV, John GR (2012). Astrocyte-derived VEGF-A drives blood-brain barrier disruption in CNS inflammatory disease. J Clin Invest 122:2454-2468.

Arion D, Unger T, Lewis DA, Levitt P, Mirnics K (2007). Molecular evidence for increased expression of genes related to immune and chaperone function in the prefrontal cortex in schizophrenia. Biol Psychiatry 62:711-721.

Barraud P, Stott S, Møllgård K, Parmar M, Björklund A (2007). In vitro characterization of a human neural progenitor cell coexpressing SSEA4 and CD133. J Neurosci Res 85:250-259.

Bernadi D, Padoan A, Ballin A, Sartori M, Manara R, Scienza R, Plebani M, Della Puppa A (2012). Serum YKL-40 following resection for cerebral glioblastoma. J Neurooncol 107:299-305.

Bigg HF, Wait R, Rowan AD, Cawston TE (2006). The mammalian chitinase-like lectin, YKL-40, binds specifically to type I collagen and modulates the rate of type I collagen fibril formation. J Biol Chem 281:21082-21095.

Bonfanti L, Peretto P (2007). Radial glial origin of the adult neural stem cells in the subventricular zone. Prog Neurobiol 83:24-36.

Bonneh-Barkay D, Wang G, Starkey A, Hamilton RL, Wiley CA (2010). In vivo CHI3L1 (YKL-40) expression in astrocytes in acute and chronic neurological diseases. J Neuroinflamm 7:34-41.

Brøchner CB, Johansen JS, Larsen LA, Bak M, Mikkelsen HB, Byskov AG, Andersen CY, Møllgård K (2012). YKL-40 is differentially expressed in human embryonic stem cells and in cell progeny of the three germ layers. J Histochem Cytochem 60:188-204.

Bystron I, Blakemore C, Rakic P (2008). Development of the human cerebral cortex: Boulder Committee revisited. Nat Rev Neurosci 9:110-122.

Chung C, Tallerico T, Seeman P (2003). Schizophrenia hippocampus has elevated expression of chondrex glycoprotein gene. Synapse 50:29-34.

Colin C, Baeza N, Bartoli C, Fina F, Eudes N, Nanni I, Martin P-M, Ouafik L, Figarella-Branger D (2006). Identification of

genes differentially expressed in glioblastoma versus pilocytic astrocytoma using Suppression Subtractive Hybridization. Oncogene 25:2818-2826.

Colton CA, Mott RT, Sharpe H, Xu Q, Van Nostrand WE, Vitek MP (2006). Expression profiles for macrophage alternative activation genes in AD and in mouse models of AD. J Neuroinflamm 3:27-38.

Correale J, Fiol M (2011). Chitinase effects on immune cell response in neuromyelitis optica and multiple sclerosis. Mult Scler 17:521-531

Craig-Schapiro R, Perrin RJ, Roe CM, Xiong C, Carter D, Cairns NJ, Mintun MA, Peskind ER, Li G, Galasko DR, Clark CM, Quinn JF, D'Angelo G, Malone JP, Townsend RR, Morris JC, Fagan AM, Holtzman DM (2010). YKL-40: A novel prognostic fluid biomarker for preclinical Alzheimer's disease. Biol Psychiat 68:903-912.

Cunningham CL, Martínez-Cerdeño V, Noctor SC (2013). Microglia regulate the number of neural precursor cells in the developing cerebral cortex. J Neurosci 33:4216-4233.

Daneman R, Zhou L, Kebede AA, Barres BA (2010). Pericytes are required for blood-brain barrier integrity during embryogenesis. Nature 468:562-566.

Faibish M, Francescone R, Bentley B, Yan W, Shao R (2011). A YKL-40 neutralizing antibody blocks tumor angiogenesis and progression: a potential therapeutic agent in cancers. Mol Cancer Ther 10:742-751.

Fossan G, Cavanagh ME, Evans CA, Malinowska DH, Møllgård K, Reynolds ML, Saunders NR (1985). CSF-brain permeability in the immature sheep fetus: a CSF-brain barrier. Brain Res 350:113-124.

Francescone RA, Scully S, Faibish M, Taylor SL, Oh D, Moral L, Yan W, Bentley B, Shao R (2011). Role of YKL-40 in the angiogenesis, radioresistance, and progression of glioblastoma. J Biol Chem 286:15332-15343.

Gadisseaux J-F, Goffinet AM, Lyon G, Evrard P (1992). The human transient subpial granular layer: an optical, immunohistochemical, and ultrastructural analysis. J Comp Neurol 324:94-114.

Garbett K, Ebert PJ, Mitchell A, Lintas C, Manzi B, Mirnics K, Persico AM (2008). Immune transcriptome alterations in the temporal cortex of subjects with autism. Neurobiol Dis 30:303-311.

García-Marqués J, López-Mascaraque L (2013). Clonal identity determines astrocyte cortical heterogeneity. Cereb Cortex 23:1463-1472.

Götz M, Huttner WB (2005). The Cell Biology of Neurogenesis. Nat Rev Mol Cell Bio 6:777-788.

Hakala BE, White C, Recklies AD (1993). Human cartilage gp-39, a major secretory product of articular chondrocytes and synovial cells, is a mammalian member of a chitinase protein family. J Biol Chem 268:25803-25810.

Hansen DV, Lui JH, Parker PRL, Kriegstein AR (2010). Neurogenic radial glia in the outer subventricular zone of human neocortex. Nature 464:554-561.

Hansen DV, Lui JH, Flandin P, Yoshikawa K, Rubenstein JL, Alvarez-Buylla A, Kriegstein AR (2013). Non-epithelial stem cells and cortical interneuron production in the human ganglionic eminences. Nat Neurosci 16:1576-1587.

He CH, Lee CG, Dela Cruz CS, Lee CM, Zhou Y, Ahangari F, Ma B, Herzog EL, Rosenberg SA, Li Y, Nour AM, Parikh CR, Schmidt I, Modis Y, Cantley L, Elias JA (2013). Chitinase 3-like 1 regulates cellular and tissue responses via IL-13 receptor α2. Cell Rep 4:830-841.

Horbinski C, Wang G, Wiley C (2010). YKl-40 is directly produced by tumor cells and is inversely linked to EGFR in glioblastomas. Int J ClinExpPathol 3:226-237.

Hormigo A, Gu B, Karimi S, Riedel E, Panageas KS, Edgar MA, Tanwar MK, Rao JS, Fleisher M, DeAngelis LM, Holland EC (2006). YKL-40 and matrix metalloproteinase-9 as potential serum biomarkers for patients with high-grade gliomas. Clin Cancer Res 12:5698-5704.

Howard BM, Mo Z, Filipovic R, Moore AR, Antic SD, Zecevic N (2008). Radial glia cells in the developing human brain. Neuroscientist 14:459-473.

Humphrey T (1966). The development of the human Hippocampal formation correlated with some aspects of its phylogenetic history. In: Hassler R, Stephan H, (eds) Evolution of the forebrain. Plenum Press, New York, p 104-116.

Iwamoto FM, Hottinger AF, Karimi S, Riedel E, Dantis J, Jahdi M, Panageas KS, Lassman AB, Abrey LE, Fleisher M, DeAngelis LM, Holland EC, Hormigo A (2011). Serum YKL-40 is a marker of prognosis and disease status in high-grade gliomas. NeuroOncol 13:1244-1251

Jacobsen M, Clausen PP, Jacobsen GK, Saunders NR, Møllgård K (1982). Intracellular plasma proteins in human fetal choroid plexus during development I. Developmental stages in relation to the number of epithelial cells which contain albumin in the telencephalic, diencephalic and myelencephalic choroid plexus. Brain Res 255:239-250.

Janas M S, Nowakowski R S, Terkelsen O B F, Møllgård K (1991). Glial cell differentiation in neuron-free and neuron-rich regions I. Anat Embryol 184:549-558.

Johansen JS, Høyer PE, Larsen LA, Price PA, Møllgård K (2007). YKL-40 protein expression in the early developing human musculoskeletal system. J Histochem Cytochem 55:1213-1228.

Johansen JS, Schultz NA, Jensen BV (2009). Plasma YKL-40: a potential new cancer biomarker? Future Oncol 5:1065-1082.

Johansen JS, Bojesen SE, Tybjærg-Hansen A, Mylin AK, Price PA, Nordestgaard BG (2010). Plasma YKL-40 and total and disease-specific mortality in the general population. Clin Chem 56:1580-1591.

Junker N, Johansen JS, Andersen CB, Kristjansen PE (2005). Expression of YKL-40 by peritumoral macrophages in human small cell lung cancer. Lung Cancer 48:223-231.

Kadhim HJ, Gadisseaux J-F, Evrard P (1988). Topographical and cytological evolution of the glial phase during prenatal development of the human brain: histochemical and electron microscopic study. J Neuropath Exp Neur 47:166-188.

Kjaergaard AD, Bojesen SE, Johansen JS, Nordestgaard BG (2010). Elevated plasma YKL-40 levels and stroke in the general population. Ann Neurol 68:672-680.

Ku BM, Lee YK, Ryu J, Jeong JY, Choi J, Eun KM, Shin HY, Kim DG, Hwang EM, Yoo JC, Park J-Y, Roh GS, Kim HJ, Cho GJ, Choi WS, Paek SH, Kang SS (2011). CHI3L1 (YKL-40) is expressed in human gliomas and regulates the invasion, growth and survival of glioma cells. Int J Cancer 128:1316-1326

Lal A, Lash AE, Altschul SF, Velculescu V, Zhang L, McLendon RE, Marra MA, Prange C, Morin PJ, Polyak K, Papadopoulos N, Vogelstein B, Kinzler KW, Strausberg RL, Riggins GJ (1999). A public database for gene expression in human cancers. Cancer Res 59:5403-5407.

Lee CG, Da Silva CA, Dela Cruz CS, Ahangari S, Ma B, Kang MJ, He CH, Takyar S, Elias JA (2011). Role of chitin and chitinase/chitinase-like proteins in inflammation, tissue-remodelling, and injury. Annu Rev Physiol 73:479-501.

Malatesta P, Hartfuss E, Götz M (2000). Isolation of radial glial cells by fluorescent-activated cell sorting reveals a neuronal lineage. Development 127:5253-5263.

Markert JM, Fuller CM, Gillespie GY, Bubien JK, McLean LA, Hong RL, Lee K, Gullans SR, Mapstone TB, Benos DJ (2001). Differential gene expression profiling in human brain tumors. Physiol Genomics 5:21-33.

Meyer G (2010). Building a human cortex: The evolutionary differentiation of Cajal-Retzius cells and the cortical hem. J Anat 217:334-343.

Møllgård K, Jacobsen M (1984). Immunohistochemical identification of some plasma proteins in human embryonic and fetal forebrain with particular reference to the development of the neocortex. Brain Res 315:49-63.

Møllgård K, Saunders NR (1986). The development of the human blood-brain and blood-CSF barriers. Neuropathol Appl Neurobiol 12:337-358.

Møllgård K, Balslev Y, Lauritzen B, Saunders NR (1987). Cell junctions and membrane specializations in the ventricular zone (germinal matrix) of the developing sheep brain: a CSF-brain barrier. J Neurocytol 16:433-444.

Nigro JM, Misra A, Zhang L, Smirnov I, Colman H, Griffin C, Ozburn N, Chen M, Pan E, Koul D, Yung WKA, Feuerstein BG, Aldape KD (2005). Integrated array-comparative genomic hybridization and expression array profiles identify clinically relevant molecular subtypes of glioblastoma. Cancer Res 65:1678-1686.

Østergaard C, Johansen JS, Benfield T, Price PA, Lundgren JD (2002). YKL-40 is elevated in cerebrospinal fluid from patients with purulent meningitis. Clin Diagn Lab Immunol 9:598-604.

Park DM, Rich JN (2009). Biology of glioma cancer stem cells. Mol Cells 28:7-12.

Pelloski CE, Mahajan A, Maor M, Chang EL, Woo S, Gilbert M, Colman H, Yang H, Ledoux A, Blair H, Passe S, Jenkins RB, Aldape KD (2005). YKL-40 expression is associated with poorer response to radiation and shorter overall survival in glioblastoma. Clin Cancer Res 11:3326-3334.

Pinto L, Götz M (2007). Radial glial cell heterogeneity–the source of diverse progeny in the CNS. Prog Neurobiol 83:2-23.

Prakash M, Bodas M, Prakash D, Nawarni N, Khetmadas N, Mandal A, Eriksson C (2013). Diverse pathological implications of YKL-40: answers may lie in outside-in signaling. Cell Signal 25:1567-1573.

Recklies AD, Ling H, White C, Bernier SM (2005). Inflammatory cytokines induce production of CHI3L1 by articular chondrocytes. J Biol Chem 280:41213-41221.

Rehli M, Krause SW, Andreesen R (1997). Molecular characterization of the gene for human cartilage gp-39 (CHI3L1), a member of the chitinase protein family and marker for late stages of macrophage differentiation. Genomics 43:221-225.

Rezaie P, Dean A, Male D, Ulfig N (2005). Microglia in the cerebral wall of the human telencephalon at second trimester. Cereb Cortex 15:938-949.

Rousseau A, Nutt CL, Betensky RA, Iafrate AJ, Han M, Ligon KL, Rowitch DH, Louis DN (2006). Expression of oligodendroglial and astrocytic lineage markers in diffuse gliomas: use of YKL-40, ApoE, ASCL1, and NKX2-2. J Neuropathol Exp Neurol 65:1149-1156.

Saunders NR, CJ Ek, Habgood MD, Dziegielewska KM (2008). Barriers in the brain: a renaissance? Trends Neurosci 31:279-286.

Schiffer D, Annovazzi L, Caldera V, Mellai M (2010). On the origin and growth of gliomas. Anticancer Res 30:1977-1998.

Shao R. 2013. YKL-40 acts an angiogenic factor to promote tumor angiogenesis. Front Physiol 4:122.

Shostak K, Labunskyy V, Dmitrenko V, Malisheva T, Shamayev M, Rozumenko V, Zozulya Y, Zehetner G, Kavsan V (2003). HC gp-39 gene is upregulated in glioblastoma. Cancer Lett 198:203-210.

Siegenthaler JA, Ashique AM, Zarbalis K, Patterson KP, Hecht JH, Kane MA, Folias AE, Choe Y, May SR, Kume T, Napoli JL, Peterson AS, Pleasure SJ (2009). Retinoic acid from the meninges regulates cortical neuron generation. Cell 139:597-609.

Siegenthaler JA, Pleasure SJ (2011). We have got you 'covered': how the meninges control brain development. Curr Opin Genet Dev 21:249-255.

Singh SK, Clarke ID, Terasaki M, Bonn VE, Hawkins C, Squire J, Dirks PB (2003). Identification of a cancer stem cell in human brain tumors. Cancer Res 63:5821-5828.

Stolp HB, Liddelow SA, Sá-Pereira I, Dziegielewska KM, Saunders NR (2013). Immune responses at brain barriers and implications for brain development and neurological function in later life. Front Integr Neurosci 7:61.

Tanwar MK, Gilbert MR, Holland EC (2002). Gene expression microarray analysis reveals YKL-40 to be a potential serum marker for malignant character in human glioma. Cancer Res 62:4364-4368.

Vasudevan A, Long JE, Crandall JE, Rubenstein JLR, Bhide PG (2008). Compartment-specific transcription factors orchestrate angiogenesis gradients in the embryonic brain. Nat Neurosci 11:429-439.

Verney C, Monier A, Fallet-Bianco C, Gressens P (2010). Early microglial colonization of the human forebrain and possible involvement in periventricular white-matter injury of preterm infants. J Anat 217:436-448.

Virgintino D, Girolamo F, Errede M, Capobianco C, Robertson D, Stallcup WB, Perris R, Roncali L (2007). An intimate interplay between precocious, migrating pericytes and endothelial cells governs human fetal brain angiogenesis. Angiogenesis 10:35-45.

Volck B, Price PA, Johansen JS, Sørensen O, Benfield TL, Nielsen HJ, Calafat J, Borregaard N (1998). YKL-40, a mammalian member of the chitinase family, is a matrix protein of specific granules in human neutrophils. Proc Assoc Am Physicians 110:351-360.

Zhang Y, Barres BA (2010). Astrocyte heterogeneity: an underappreciated topic in neurobiology. Curr Opin Neurobiol 20:588-594.